An Optimized Purification and Reconstitution Method for the MscS Channel: Strategies for Spectroscopical Analysis†

Valeria Vásquez,‡,§ D. Marien Cortes,§ Hiro Furukawa,|| and Eduardo Perozo*,§

Department of Molecular Physiology and Biological Physics, University of Virginia, Charlottesville, Virginia 22908, Institute of Molecular Pediatrics Science and Department of Biochemistry and Molecular Biology, Pritzker School of Medicine, University of Chicago, Chicago, Illinois 60637, and Vollum Institute/Oregon Health and Science University, Portland, Oregon 97239

Received February 15, 2007; Revised Manuscript Received March 21, 2007

ABSTRACT: The mechanosensitive channel of small conductance (MscS) plays a critical role in the osmoregulation of prokaryotic cells. The crystal structure of MscS revealed a homoheptamer with three transmembrane segments and a large cytoplasmic domain. It has been suggested that the crystal structure depicts an open state, but its actual functional conformation remains controversial. In the pursuit of spectroscopical approaches to MscS gating, we determined that standard purification methods yield two forms of MscS, with a considerable amount of unfolded channel. Here, we present an improved high-yield purification method based on *Escherichia coli* expression and a biochemical characterization of the reconstituted channel, optimized to yield approximately 4 mg of a single monodisperse product. Upon reconstitution into lipid vesicles, MscS is unusually prone to lateral aggregation depending on the lipid composition, particularly after sample freezing. Strategies for minimizing MscS aggregation in two dimensions for spectroscopic analyses of gating have been developed.

Mechanotransduction plays an important role in a wide range of physiological processes such as touch, pain, hearing, balance, proprioception, blood pressure regulation, turgor control in plant cells, and regulation of cell volume. It has been suggested that mechanosensitive channels might have evolved as cellular osmoregulators that sensed changes in the concentration of water across bacterial membranes (*1*−*7*). Mechanosensitive channels belong to a structurally heterogeneous group and have been classified according to their function rather than topology. The group includes members of the two-pore domain potassium channel (*8*, *9*), the amiloride-sensitive sodium channel (*10*), the TRP channels (*11*), and the prokaryotic mechanosensitive channels (*12*).

The prokaryotic mechanosensitive channels are key components in the emergency response of prokaryotes to sudden osmotic downshock (*13*, *14*). These channels are classified according to their conductance and to the amount of tension needed to activate them as MscL, MscS, and MscM (mechanosensitive channel of large, small, and mini conductance, respectively). In particular, MscL and MscS have been shown to play a critical role in osmoregulation, since cells lacking mechanosensitive channels lyse upon osmotic downshock (*13*). Over the past several years, a considerable amount of functional and structural information has been gathered on the prokaryotic mechanosensitive channel family. Electrophysiological and spectroscopical approaches have provided information about their conductance properties and activation process (*12*, *15*−*18*). The crystal structures of MscL and MscS have revealed their three-dimensional structure (*19*, *20*) and a critical starting point for mechanistic interpretations. Still, the gating mechanism in either of these channels is not fully understood.

MscS (Figure 1A) belongs to a large and widespread family of membrane proteins (*21*), which is distributed among prokaryotes, archaea, and plants (*22*, *23*), in which function is defined by interaction with the lipid bilayer and as such represents an ideal model system for studying the biophysical basis of mechanotransduction. Besides, protein−membrane interactions are not unique to mechanosensitive channels since the open probability of several other ion channels is modulated via membrane stretch or membrane composition (*24*−*27*). A high-quality biochemical preparation is required to routinely express and purify (at milligram levels) MscS from *Escherichia coli*, which might help increase crystal resolution and allow efforts aimed at the elucidation of the molecular mechanisms of tension-dependent gating. Here, we present a new approach for high-level expression and purification of several MscS constructs in different *E. coli* strains. We also present a strategy for reconstituting MscS in liposomes that avoids its natural tendency to aggregate in the plane of the bilayer. These methodologies will play a key role in our attempts to understand the molecular basis of the MscS gating mechanism.

† This work was supported by National Institutes of Health Grant GM063617 to E.P.

* To whom correspondence should be addressed. E-mail: eperozo@uchicago.edu. Phone: (773) 834-4734. Fax: (773) 834-4632.

‡ University of Virginia.

§ University of Chicago.

|| Vollum Institute/Oregon Health & Science University.

10.1021/bi700322k CCC: $37.00
Published on Web 05/15/2007

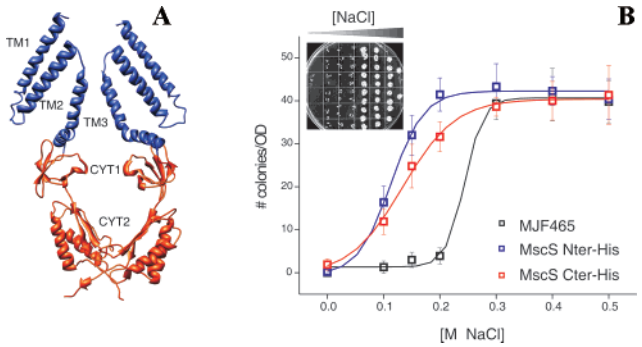

FIGURE 1: Functional characterization of different MscS constructs. (A) Ribbon representation of MscS showing two subunits of the heptamer. TM helices are colored blue and cytoplasmic (CYT) domains red. (B) Viability assay of MscS constructs upon osmotic downshock, following the protocol of Batiza et al. (*14*). The downshock was made by diluting the cells in various shock media ranging from 0 to 500 mM NaCl. The MJF465 strain (black curve) was used as a negative control since it lacks native mechanosensitive channels. The blue curve represents MscS expressed in pQE32 with six histidines at the N-terminus, and the red curve represents MscS expressed in pQE70 with six histidines at the C-terminus. The inset shows a representative result for MJF465 cells after a downshock assay.

EXPERIMENTAL PROCEDURES

Materials. MJF429 (Frag1, Δ*yggB*, Δ*kefA*) and MJF465 (Frag1, Δ*mscL*, Δ*yggB*, Δ*kefA*) (*13*) were kindly donated by I. R. Booth from the University of Aberdeen (Aberdeen, U.K.). *E. coli* Rosetta and the vector pET28a were purchased from Novagen (San Diego, CA). *E. coli* M15, SG1300, and the vectors pQE32 and pQE70 were bought from QIAGEN (Valencia, CA). The IPTG[1] and the detergents Fos-Choline 14 (solubilization grade) and DDM (solubilization grade) were obtained from Anatrace (Maumee, OH). Talon cobalt resin was bought from Clontech (Mountain View, CA). The reducing agent TCEP was purchased from Pierce (Rockford, IL). The reducing agent TCYP, along with the fluorophores fluorescein 5-maleimide and tetramethylrhodamine 5-maleimide, was bought from Molecular Probes (Carlsbad, CA). The spin-label was purchased from Toronto Research Chemicals Inc. (North York, ON). The lipids DOPC, POPG, POPE, and *E. coli* polar lipid extract were bought from Avanti Polar Lipids Inc. (Alabaster, AL). All other reagents were purchased from Sigma or Fisher.

Construct and Strains. A 600 ng amount of *E. coli* genomic DNA was used as a template for PCR. The resultant product (846 bp) was gel purified and cloned in pQE32 and in pET28a, vectors containing a His_6 epitope at the N-termini, and in pQE70, in which the His_6 epitope was at the C-terminus. MscS-pQE32 and MscS-pQE70 were used to express the channel in *E. coli* M15, SG1300, MJF429, and MJF465; MscS-pET28 was used for expression in *E. coli* Rosetta.

[1] Abbreviations: CW-EPR, continuous-wave electron paramagnetic resonance; DDM, *n*-dodecyl β-D-maltopyranoside; DOPC, 1,2-dioleoyl-*sn*-glycero-3-phosphocholine; IPTG, isopropyl β-D-thiogalactopyranoside; PBS, phosphate-buffered saline; PMSF, phenylmethanesulfonyl fluoride; POPE, 1-palmitoyl-2-oleoyl-*sn*-glycero-3-phosphoethanolamine; POPG, 1-palmitoyl-2-oleoyl-*sn*-glycero-3-[phospho-*rac*-(1-glycerol)]; spin-label, (1-oxyl-2,2,5,5-tetramethylpyrrolidin-3-yl) methyl methanethiosulfonate; TCEP, tris(2-carboxyethyl)phosphine hydrochloride; TCYP, tris(2-cyanoethyl)phosphine; TM, transmembrane.

Functional Assay. Downshock assays were developed as described in ref *14*, with the following modifications. Cultures growing in LB and 500 mM NaCl were induced at an OD_{600} of 0.6 with 1 mM IPTG; after being induced for 1 h, the cells were adjusted to an OD_{600} of 1.0, pelleted down, and then resuspended in 50 μL of fresh LB and 500 mM NaCl. The downshock was made by diluting the cells 1:40 in various shock media ranging from 0 to 500 mM NaCl (pH 7). After 5 min, the cells were serially diluted, and 5 μL aliquots were plated on LB agar. Plated cells were grown overnight, and the colonies were counted and normalized against the OD_{600} (measured right before the downshock).

Expression and Purification of MscS in E. coli Cells. Fresh competent cells were transformed with the desired construct, and the transformation mixture was grown overnight in the presence of the proper antibiotics. The cells were diluted 1:100 in regular LB medium and grown at 37 °C to an OD_{600} of 1.0−1.2, and protein expression was induced with the addition of 0.8 mM IPTG in the presence of 0.4% glycerol for 4 h at 26 °C. The cells were harvested and homogenized (high-pressure homogenizer, EmulsiFlex-C3) immediately, in the presence of PBS and 1 mM PMSF (*28*). The membranes were spun down at 100,000*g* for 30 min, and the pellet was resuspended in PBS and PMSF. Solubilization was carried out with 1% Fos-Choline 14 (*20*), in the presence of 10% glycerol in PBS and PMSF, at pH 7.5, overnight at 4 °C; solubilization with 6 mM DDM resulted in a significantly lower protein yield. This homogenate was spun down at 100,000*g* for 30 min, and the supernatant was incubated with cobalt resin for 3 h at 4 °C. The resin was washed with 1 mM DDM (regardless of initial detergent) and 10% glycerol in PBS buffer (pH 7.5; 10 times the resin volume), then with the same buffer at pH 6 (10 times the resin volume), and the final wash was made with 5 mM, 1 mM DDM, and 10% glycerol in PBS buffer (pH 6; 25 times the resin volume). The channel was eluted with 300 mM imidazole, 1 mM DDM, and 10% glycerol in PBS buffer (pH 6). The typical yield of WT MscS was ∼4 mg for M15, SG1300, and Rosetta and ∼2 mg for MJF429 and MJF465 per liter of LB culture. When MscS Cys mutants were purified for fluorescence or CW-EPR measurements, washing buffers were degassed and contained 0.5 mM TCEP and 0.5 mM TCYP. To check the oligomeric state of the protein, samples were run in a Superdex 200 HR 10/30 column (Amersham Biosciences, Uppsala, Sweden) and monitored in an AKTA FPLC system (model P-920) from the same company.

Mass Determination by Static Light Scattering. The purified MscS was run on a Superdex 200 HR 10/30 column coupled to a light scattering system, with a refractive index (Wyatt Technology Corp.) and UV (Shimadzu) detectors. The system was equilibrated with a buffer containing 1 mM DDM, 1 mM EDTA, 150 mM NaCl, and 20 mM Hepes (pH 7). The light scattering was measured using a linearly polarized GaAs laser at 690 nm (λ) from 57° to 126° by nine detectors. The increment of refractive index over the increment of protein concentration for the protein−detergent complex, $(dn/dc)_{pd}$, was first determined using the following equation:

$$(dn/dc)_{pd} = (k_2 \epsilon RI)/UV$$

where ϵ is the extinction coefficient of the protein at 280

nm (mg^{-1} mL cm^{-1}), RI is the value of the refractive index, and UV is the absorbance at 280 nm. The k_2 value was determined using a standard curve from soluble standard proteins (bovine albumin, β-amylase, and apoferritin F; Sigma) whose d*n*/d*c* is constant at 0.187 mL/g. Using the experimentally determined $(dn/dc)_{pd}$ value (0.24), the protein molecular weight was determined from the Debye plot, where the intensity of light scattering is plotted against the scattering angle (ASTRA software, Wyatt Technology Corp.).

MscS Reconstitution. After purification, MscS was reconstituted in preformed liposomes following the protocol described in ref *29*. For electrophysiological measurements, MscS was reconstituted in a protein:lipid ratio of 1:200 (mass to mass). For CW-EPR and FRET experiments, the reconstitution ratio was 1:750 (mole to mole). For patch-clamp experiments, the lipids were resuspended in HEPES buffer (pH 7.5) for fluorescence and EPR measurements, and the lipids were resuspended in PBS (pH 7.5). In either case, the dilution method (to decrease the DDM concentration below its CMC), in the presence of Bio-beads, was used to incorporate the channels into the liposomes. After incubation for 3−10 h with Bio-beads (unless explicitly stated), the proteoliposomes were pelleted down at 100,000*g*, resuspended, and used for spectroscopic measurements; for electrophysiological measurements, they were subjected to a dehydration−rehydration cycle as previously described (*30*, *31*).

Liposome Patch Clamp. Single-channel currents were obtained in the inside-out configuration under symmetrical (200 mM KCl, 90 mM $MgCl_2$, 10 mM $CaCl_2$, and 5 mM HEPES) and asymmetrical conditions (100 mM KCl in the pipette and 300 mM KCl in the bath, with all of the other salts kept constant), at pH 6. The pipettes were obtained out of glass capillaries and were fire-polished before they were used, until a resistance between 2 and 2.5 MΩ was reached. Negative pressure on the patch was obtained by applying suction through a syringe and monitored with a homemade piezo-electric pressure transducer. Single-channel and macroscopic currents were recorded with a DAGAN 3900 patch-clamp amplifier, and currents were sampled at 10 kHz with an analog filter set to 2 kHz. Single-channel analyses were conducted using pCLAMP9 (Axon Instruments) (*32*).

EPR Spectroscopy and Analysis. MscS-Cys mutants were purified and spin-labeled using a 1:10 molar excess of the label. After reconstitution, their spectra were obtained at room temperature in a Bruker EMX X-band EPR spectrometer, and the mobility of the probe was obtained from the inverse central line width of the EPR spectrum (ΔH_o^{-1}) (*29*).

Fluorescence Spectroscopy. For FRET experiments, single MscS-Cys mutants were purified and labeled with fluorescein and tetramethylrhodamine, at a 1:10 molar ratio (monomer: fluorophore) following ref *33*. After the samples were reconstituted, measurements were taken in a Shimadzu 1501 spectrofluorimeter.

RESULTS

Functional Characterization of His-Tagged MscS Constructs. MscS was cloned in several vectors that mainly differ in the position of the His tag. To test the functional behavior of these constructs, a downshock assay was carried out in MJF465, an *E. coli* strain that lacks genomic MscL, MscS, and MscK. Figure 1B illustrates a typical survival experiment (*13*, *14*) in which the cells are exposed to a sudden reduction of the external osmolarity. MJF465 was used as a negative control because it does not survive under extreme hypotonic conditions ($[NaCl]_{1/2} = 0.24 \pm 0.01$, black trace). We did not find major differences in the midactivation point of MscS with six histidines at the N-terminus ($[NaCl]_{1/2} = 0.11 \pm 0.005$, blue trace) and MscS with six histidines at the C-terminus ($[NaCl]_{1/2} = 0.13 \pm 0.007$, red trace); both of the constructs were able to protect the cell against hypoosmotic challenge.

The Oligomeric Behavior of MscS Depends on Purification Conditions. The purification methodology presented in this paper enables production of MscS at milligram scale in detergent solutions. In an effort to develop a one-step purification method suitable for labeling and spectroscopy studies, we tested the procedures already available in the literature. Using the protocol previously described by Bass et al. (*20*), we were unable to obtain single monodisperse peaks by the exclusion chromatography method (skipping the anion exchange), as shown in Figure 2A (red trace; N-ter His Crystal refers to the conditions that were used for crystallography). The purification protocol of Sukharev (*31*), which includes solubilization with OG and purification with a mixture of OG-asolectin, yielded unexpectedly small amounts of the putative heptamer (see the column labeled OG purification in Figure 2C), and the chromatogram showed additional peaks (data not shown).

Our failure to generate a consistent monodisperse peak with either of these methods prompted us to pursue an alternative protocol. Cultures were grown in LB medium (instead of Terrific Broth medium) at 37 °C up to an OD_{600} of 1.0−1.2, and induction of MscS was carried out with 0.8 mM IPTG in the presence of 0.4% glycerol at 26 °C (different IPTG and glycerol concentrations strongly reduced the protein yield). Cells were homogenized after induction for 4 h, a key step to increase the yield of the monodisperse peak. Glycerol (10%) was used in the purification buffers to increase the amount of functional channel. No significant differences were observed between cold purifications and room-temperature ones. Finally, although gel filtration chromatography on Superdex 200 can be used as an additional cleanup step, we have found this not to be necessary unless we are evaluating a new condition or construct.

Once we obtained a single monodisperse peak of MscS from the same construct that was used for the crystal trials (Figure 2A, black trace, N-ter His), the same purification protocol was used for the construct with the His tag at the C-terminus. Surprisingly, the main peak of the C-ter His construct (Figure 2B, 12.6 mL elution volume, red trace) was significantly shifted from that of the N-ter His (Figure 2A,B, 11.3 mL, black trace) even though the latter has only 12 additional residues. Both constructs were quite stable in solution even after several weeks of storage at 4 °C; however, the N-ter His construct could be stored for up to 3 months, whereas the C-ter His unfolds after 4 weeks (data not shown). The long stability of both constructs makes them suitable for crystal trials.

A summary of all the different cells, constructs, detergents, and conditions tried for MscS purification is shown in Figure 2C. The efficiency of each condition was determined by comparing the relative amount of large oligomer (presum-

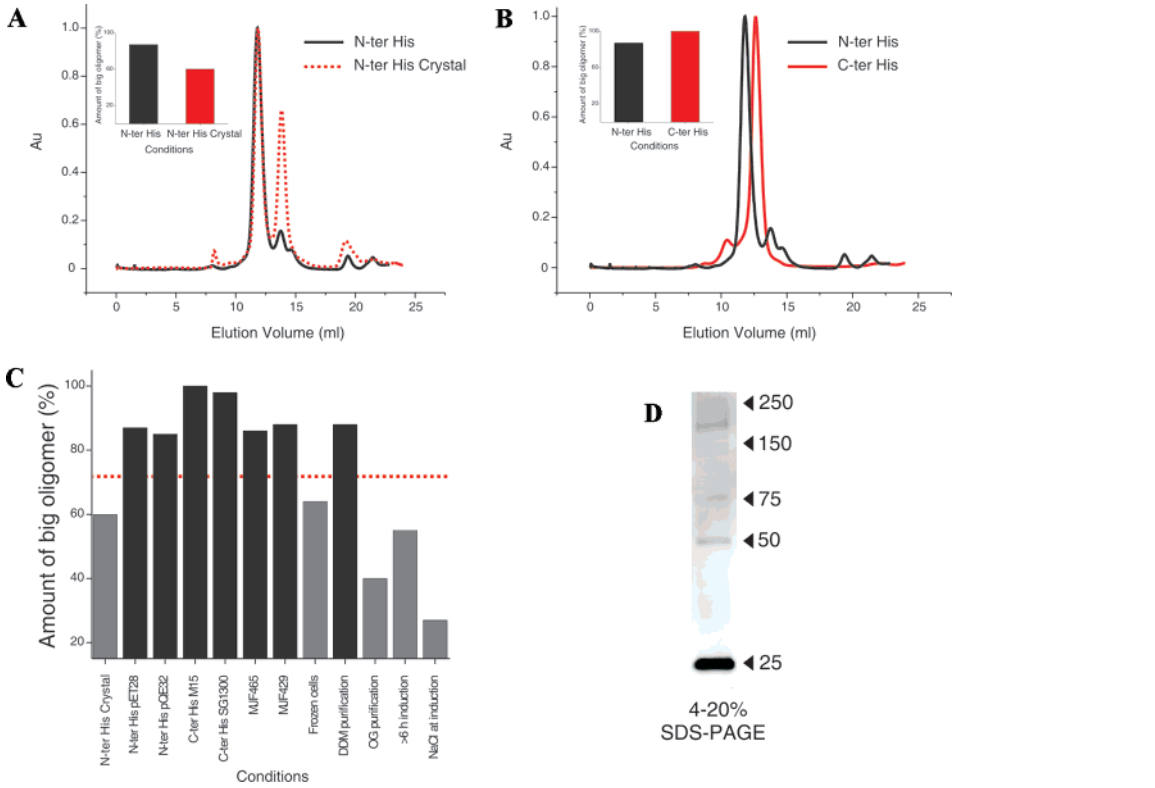

FIGURE 2: Evaluation of different MscS constructs and purification conditions. (A) Gel filtration chromatogram of MscS-pET28 expressed in Rosetta cells. Comparison of the purification of MscS constructs containing six histidines with 12 amino acid residues at the N-terminus (pET28 vector in Rosetta cells). The black (N-ter His) curve represents the conditions under which MscS is induced with the addition of 0.8 mM IPTG and 0.4% glycerol at 26 °C for 4 h, and the purification buffers containing 10% glycerol. The red dashed line (N-ter Crystal) corresponds to induction of MscS with 1 mM IPTG at 37 °C for 2 h. The inset represents the amount of putative heptamer per preparation that was obtained for both conditions. (B) Comparison of two different MscS constructs using the first condition described above (in both cases). The black curve represents the construct with six histidines with 12 amino acid residues at the N-terminus, and the red curve represents the one with six histidines at the C-terminus (pQE70 vector in M15 cells). The inset shows the amount of putative heptamer per preparation that was obtained for both constructs. (C) Yield of purified oligomeric MscS obtained from the expression in different *E. coli* cells and from variations in the purification protocol, evaluated from the elution time in a gel filtration column. The red dashed line denotes those conditions that give less than 70% of the large oligomer. (D) Oligomeric behavior of purified MscS exhibited in a SDS−PAGE Coomassie-stained gel. The 4 to 20% gradient gel shows four possible oligomeric states of MscS after purification; molecular mass (kilodaltons) markers are shown at the right.

ably heptamer) obtained per preparation. We found that freezing the cells (not the membranes), longer induction times, or even inducing in the presence of 500 mM NaCl diminished the amount of the large oligomer peak (gray bars). Unexpectedly, we could not obtain a stable protein preparation when we solubilized and purified our constructs with OG, a detergent widely used in the solubilization of integral membrane proteins and also used for other MscS constructs as previously described (*31*). Solubilization with Fos-Choline 14 or DDM yields, in both cases, a very stable preparation, the only difference being the amount of protein obtained (twice as much for Fos-Choline 14). The best results with regard to oligomeric stability and protein yield were obtained with systems in which *E. coli* was tightly regulated (pET and pQE systems) and no protein leak was present (data not shown).

Figure 2D shows the SDS−PAGE profile corresponding to the first peak in the gel filtration chromatogram (11.3 mL elution volume in Figure 2A). Four major bands, possibly corresponding to the heptamer (∼200 kDa), trimer (∼75 kDa), dimer (∼50 kDa), and monomer (∼25 kDa) of MscS, were observed. At 25 kDa, MscS in SDS−PAGE gels runs smaller than its theoretically predicted molecular mass (31 kDa). This behavior was previously reported by a number of labs (*31*, *34*−*36*). It is noteworthy that MscS, after purification, has some level of resistance to SDS, a strong anionic detergent that promotes oligomer dissociation in most membrane proteins. When the sample corresponding to the second peak in Figure 2A (13.8 mL elution volume) was run, only bands that might correspond to the dimer and the monomer were observed (data not shown). The difference between the two fractions is not due to proteolysis, since mass spectrometry (MS/MS) showed that there were no changes in amino acid content for the monomer.

To further evaluate the hydrodynamic behavior of the purified protein, we used light scattering/refractive index analysis to accurately determine the absolute molecular mass of heptameric MscS, under native conditions. The sample corresponding to the 11.3 mL fraction of the Superdex column (Figure 2A) was homogeneous in size, and its mass was 220 kDa. This measurement indicates that we have the proper assembly for the heptamer since the theoretical molecular mass of the monomer is 30,896 Da (Figure 3). On the other hand, the refractive index and UV values for the 13.8 mL sample (Figure 2A) were off and close to the detergent micelle peak (*37*) so that we could not precisely determine its exact mass. However, a rough estimate of ∼50 kDa suggests the presence of a mixed population of

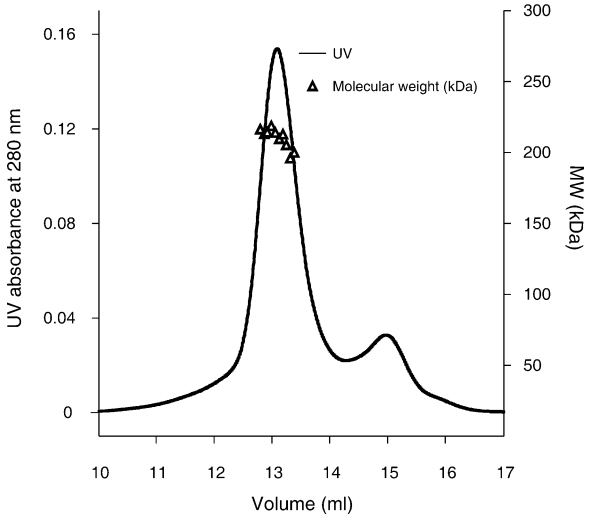

FIGURE 3: Determination of masses of purified MscS through ASTRA software analysis (Wyatt Technology Corp.) of SEC-LS/UV/RI data. The calculated molecular mass value for heptameric MscS (triangles) is plotted. The solid line corresponds to the UV trace of MscS eluting from the SEC column.

monomer, dimer, and micelle. We have found that, in a manner independent of the construct and the strain, the second peak (13.8 mL, Figure 2A) essentially disappears when the induction temperature is 26 °C, IPTG levels are less than 1 mM, glycerol is kept throughout the induction and purification, the induction time does not exceed 5 h, and, more importantly, the cell rupture occurs immediately after the cells are harvested. We found that some cysteine mutants promote dissociation of the heptamer into an unfolded channel, particularly cysteine substitutions on the TM3 segment (positions 93−101, 107, and 115) which are located along the channel 7-fold axis of symmetry.

Functional Behavior of the Purified Channel. We assessed MscS functionality after lipid reconstitution using the patch-clamp technique. Gel filtration fractions corresponding to the heptamer and the small oligomer were reconstituted in *E. coli* polar lipids, at a 1:200 protein:lipid mass ratio. For the 11.3 mL peak, shown in Figure 2A (heptamer, Figure 4B), we found the same conductance reported elsewhere (1 nS) under symmetric and asymmetric conditions (*16*, *31*, *32*, *38*). However, we were unable to detect current activity out of the reconstituted 13.8 mL peak (Figure 2A), even though the protein was well reconstituted as suggested by delipidation experiments (data not shown). These results imply that the second peak (Figure 2A) derives from an unfolded or partially assembled channel (Figure 4C).

Two-Dimensional Aggregation of Reconstituted MscS. For membrane proteins, aggregation is a critical issue, since spectroscopic measurements of local dynamics and solvent accessibility are dependent on the channel being monodisperse on the plane of the bilayer. Two-dimensional aggregation has been reported for ion channels (*33*, *39*) and other membrane proteins (*40*, *41*). To check if MscS tends to aggregate in DOPC membranes, we mutated residues to cysteine and spin-labeled 21 residues (Figure 5A) on the TM1 segment (the most exposed TM segment) to analyze its mobility profile. Figure 5B clearly shows the differences found in local dynamics between the peripheral TM segments in MscL (TM2) (*42*) and MscS (TM1). The difference in average mobility for both TM segments (0.16 for MscS and

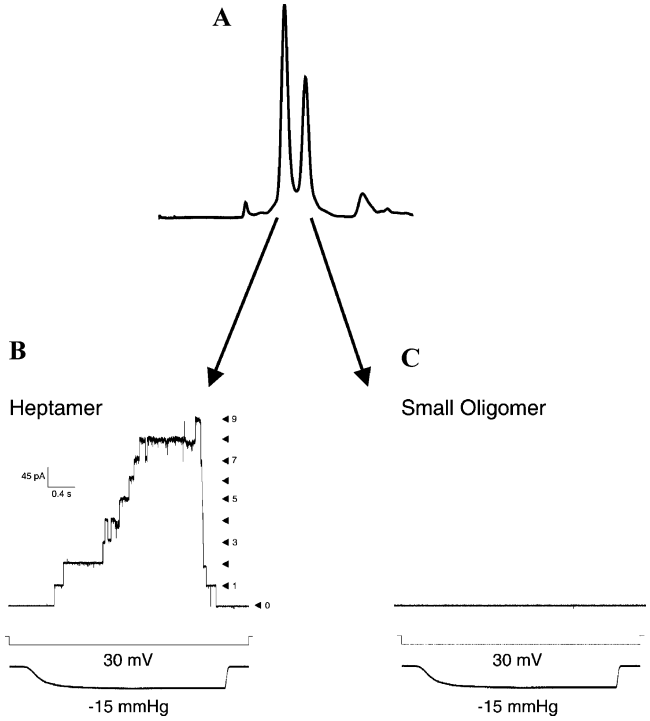

FIGURE 4: Single-channel records from purified MscS in asymmetric solutions (100 mM KCl pipette and 300 mM KCl bath at pH 6.0). Channel activity was elicited by applying negative transbilayer pressure under patch-clamp conditions. (A) Elution profile of MscS when the two kinds of oligomers are present in the purification. The arrows point to the fractions that were reconstituted in preformed liposomes. (B) Representative single-channel traces of purified and reconstituted heptameric MscS in liposomes made with *E. coli* polar lipids in a protein:lipid ratio of 1:200 (mass to mass). (C) Reconstitution of small oligomer yields no activity under the same conditions as in panel B.

0.22 for MscL) suggests that there is a limited lipid−protein interface for MscS, typical of aggregated samples (*33*). MscS aggregation was also apparent when we compared this data set with peripherally located TM segments of ion channels known to be monodisperse, such as TM1 in KcsA (*29*), and S3 and S4 in KvAP (*33*).

To decrease the level of aggregation in DOPC vesicles, we included in the mixture POPG, reported to reduce the level of aggregation in KvAP proteoliposomes (*33*). Addition of POPG to the liposomes (6:1 DOPC:POPG) resulted in more mobile EPR spectra (Figure 5C). When we plotted the mobility profiles for MscS reconstituted in DOPC (gray trace) and in DOPC and POPG (black trace), there were large differences in spin-label dynamics (Figure 5D), and the average mobility for the latter was similar to the averages reported for other peripheral TM segments. The fact that the average mobility is high, with few motionally restricted positions, indicates that this TM segment is not tightly packed against the rest of the protein.

We further investigated this phenomenon using reconstituted channels labeled with either fluorescein or tetramethylrhodamine, at positions that are putatively exposed to the membrane (Figure 6A). When these two labeled populations are mixed before reconstitution, channels that aggregate in liposomes should produce a strong FRET signal but monodisperse channels should not. Using this readout, we determined that aggregation is critically dependent on the type of lipid used (Figure 6B), as well as on the protein:

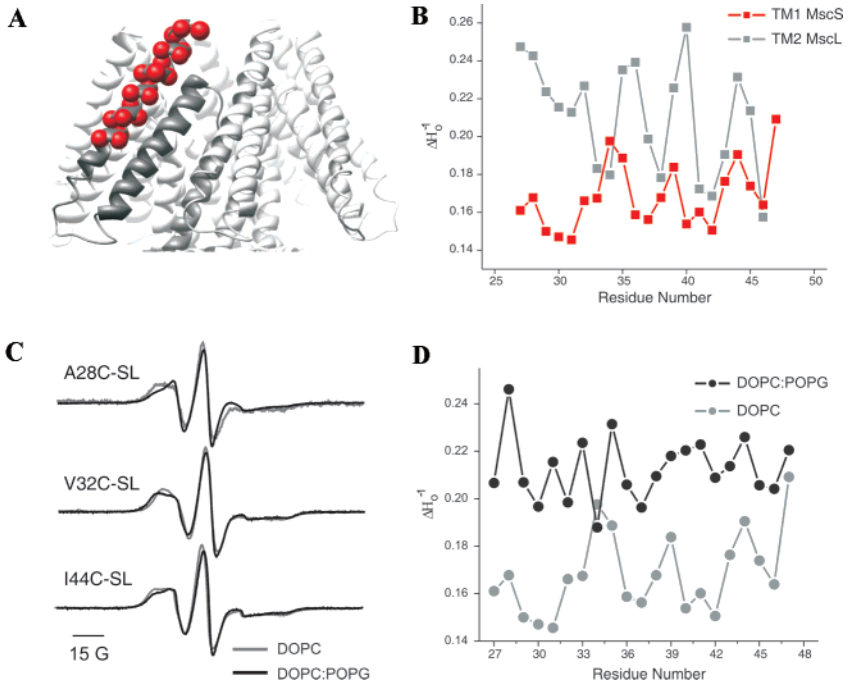

FIGURE 5: MscS mobility profiles monitored by CW-EPR from spin-labels attached to Cys residues in TM1. (A) Ribbon diagram of the TM segments of MscS showing in red spheres the TM1 residues that were mutated to cysteine and spin-labeled. (B) Aggregation was detected by comparing the mobility (ΔH_o^{-1}) profiles obtained for TM1 in MscS (red trace) and TM2 in MscL (gray trace); both channels were reconstituted in DOPC vesicles. (C) Representative first-derivative EPR spectra of spin-labeled mutants (A28C, V32C, and I44C), reconstituted in DOPC (gray spectra) and in DOPC:POPG liposomes (3:1 ratio, black spectra). (D) Comparison of mobility (ΔH_o^{-1}) profiles between MscS reconstituted in DOPC:POPG liposomes (black trace) and in DOPC vesicles (gray trace).

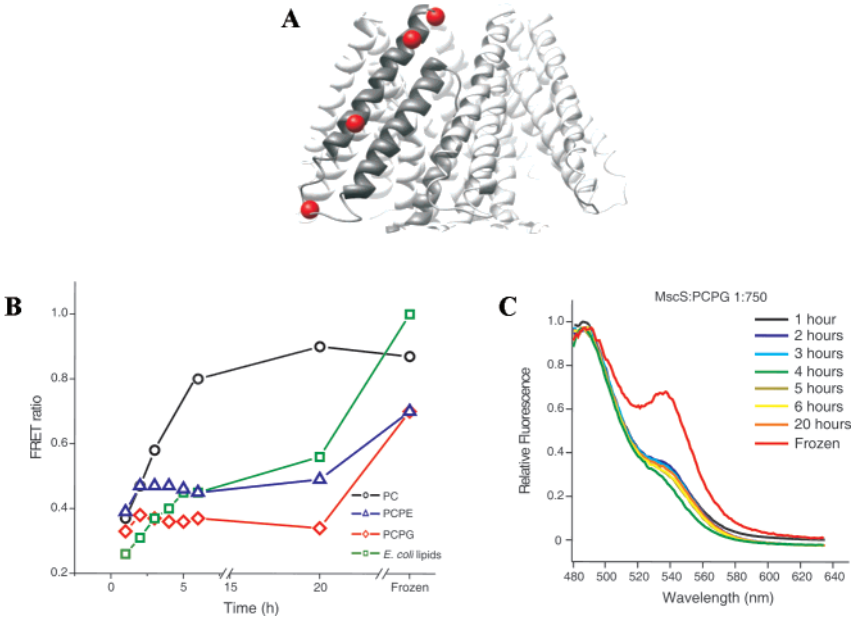

FIGURE 6: MscS two-dimensional aggregation in liposomes measured by fluorescence energy transfer (FRET), after co-reconstitution of channels labeled with fluorescein and tetramethylrhodamine. Excitation was at 491 nm and emission collected from 480 to 660 nm. (A) Ribbon diagram of the TM segments of MscS showing in red spheres the Cys residues that were labeled with two different fluorophores (Y27C, V32C, R46C, and R59C). (B) Aggregation time course in several systems of lipids: DOPC (PC, black trace), DOPC:POPE (PCPE, blue trace), DOPC:POPG (PCPG, red trace), and *E. coli* polar lipid extract (*E. coli* lipids, green trace). (C) Aggregation profile for MscS in DOPC:POPG liposomes, reconstituted in a 1:750 protein:lipid molar ratio. Measurements were taken at different times after reconstitution and also after the reconstituted samples were frozen.

lipid ratio of the reconstitution, since a molar ratio higher than 1:750 produced aggregation (data not shown). As expected from the EPR results, MscS reconstituted in DOPC membranes (PC, black trace) shows significant FRET signals within 3 h at room temperature and is fully aggregated overnight. The presence of anionic lipids in the mixture is required, since DOPC:POPE proteoliposomes (PCPE, blue trace) help reduce the level of aggregation, while DOPC:POPG (PCPG, red trace) proteoliposomes did not show aggregation at all, unless the samples were frozen (Figure 6B,C). Freezing the samples promoted aggregation, under most conditions, in a manner independent of the lipid

mixture used in the reconstitution. FRET signals were also found after reconstitution in *E. coli* polar lipids extract (green trace), but the magnitude was not as high as that of the DOPC signal.

DISCUSSION

Prokaryotic mechanosensitive channels represent a unique model system for studying the molecular basis of mechanotransduction and the role of lipid−protein interactions in membrane protein function. With recent advances in membrane protein crystallization, structures are being obtained at an unprecedented rate, yet as demonstrated, complementary dynamic information is required to ultimately understand the membrane protein functional mechanism, in addition to the structure (*18*, *43*).

Our first step prior to purification was to test the function of our constructs. Even though both constructs were functional, the ability of the C-terminal His tag construct of MscS to protect the cell from the downshock seems to be weaker than that of the construct with the N-terminal His tag. A study by Schumann and collaborators (*36*) on the carboxy terminus showed that alterations on this domain affect the recovered activity of MscS after the first pulse of tension, under patch-clamp conditions. The mechanism by which the presence of the histidines at the end of the barrel alters the response of MscS to sudden osmotic changes remains unknown.

Here, we have developed and optimized a one-step protocol for routinely purifying large quantities of functional MscS. In a manner independent of the construct or the *E. coli* strain, we found that the key steps in obtaining a single monodisperse peak of heptameric MscS are (1) low-temperature induction, (2) a low IPTG concentration, (3) addition of glycerol during expression and subsequent purification, (4) short induction times, and (5) cell rupture immediately after harvesting. An important feature of this purification protocol is that the channel remained monodisperse after several weeks of storage at 4 °C, and the purification tags did not interfere with the assembly or oligomeric state of MscS.

However, we were surprised by the small amount of heptamer obtained when the cells were induced in the presence of 0.5 M NaCl. Stokes et al. (*44*) were able to measure an increment of expression on genomic MscS and MscL when the cells were grown under high-osmolarity conditions. In our hands, while the yield increased, only 25% (Figure 2C) of the total amount of channel expressed was in the heptameric form. This might be due to the fact that with NaCl the stress sigma factor RpoS is upregulated (*44*). Thus, by increasing the amount of genomic MscS in the preparation along with the increment of plasmidic MscS (IPTG-inducible), a heterogeneous population of channels decreased the yield of total heptamer.

In spite of its low yield, expressing MscS in *E. coli* strains such as MJF455 or MJF465 is an important requirement for obtaining a homogeneous preparation of channels suitable for crystallization. Since electrophysiological analysis has suggested that each *E. coli* cell expresses ∼140−210 MscS monomers (*44*), it is very likely that the MscS population used in the crystal trials was a mixed one, with the contribution of channels with a histidine tag coming from the plasmid and without a tag coming from the genome.

Previous electrophoretic analysis of membrane preparations and purified channel showed that MscS monomer migrates as a 25−30 kDa band (*31*, *34*) and that the heptamer can only be observed in the presence of chemical cross-linkers, or using LDS detergent as recently shown in ref *45*. We were surprised to see the heptamer on SDS−PAGE gels after purification (Figure 2D), since most membrane proteins tend to fully dissociate even at very low concentrations of SDS; however, oligomeric stability for harsh detergents has been observed for other membrane proteins like glycophorin A (*46*) and KcsA (*28*). Sukharev has also reported that even without the cross-linker (DSS) MscS exhibits a small amount of dimer (*31*). We also found that a fraction of MscS dimer (along with the monomer) was always present on the electrophoresis gels, even under the harshest conditions.

Mechanosensitive channel function relies on their interaction with the membrane, making reconstituted systems a requisite for their study (*18*, *43*, *47*). The ability to reconstitute MscS in liposomes allows experimental control of intrabilayer forces using a variety of lipid mixtures and conditions that have specific influence over the TM pressure profile and thus influence channel conformation. Here, we offer a reliable purification system along with the characterization of MscS in liposomes that will open the door to the application of multiple structural approaches. Our electrophysiological results, in *E. coli* polar lipids, are in agreement with previous reports regarding single-channel conductance and inactivation (*32*, *38*).

The determination of the topology and three-dimensional architecture of membrane proteins by spectroscopic approaches relies on the fact that proteins have to be monodisperse on the plane of the bilayer; otherwise, the acquired information will be affected by expurious protein−protein contacts, especially on those segments that are at the periphery of the molecule. The results obtained from EPR and FRET experiments show that the lipid systems commonly used for electrophysiological measurements, such as DOPC or *E. coli* polar lipids, cannot be used for MscS structural determination, since they promote two-dimensional aggregation of MscS. Perhaps MscS aggregation naturally occurs in *E. coli* membranes, and it might be essential for its function; however, more studies are required to assess this phenomenon.

ACKNOWLEDGMENT

We thank Randal Bass, Julio Cordero-Morales, Luis Cuello, Christopher Ptak, Sudha Chakrapani, and Vishwanath Jogini for providing comments and experimental advice, Julio Cordero-Morales and Marcos Sotomayor for critically reading the manuscript, and Eric Gouaux for generous access to his light scattering system. We also thank the W. M. Keck Biomedical Mass Spectrometry Laboratory and the University of Virginia Biomedical Research Facility, which are funded by a grant from the University of Virginia Pratt Committee.

REFERENCES

1. Batiza, A. F., Rayment, I., and Kung, C. (1999) Channel gate! Tension, leak and disclosure, *Structure 7*, R99−R103.
2. Hamill, O. P., and Martinac, B. (2001) Molecular basis of mechanotransduction in living cells, *Physiol. Rev. 81*, 685−740.

3. Martinac, B. (2001) Mechanosensitive channels in prokaryotes, *Cell. Physiol. Biochem. 11*, 61−76.
4. Blount, P. (2003) Molecular mechanisms of mechanosensation: Big lessons from small cells, *Neuron 37*, 731−734.
5. Martinac, B. (2004) Mechanosensitive ion channels: Molecules of mechanotransduction, *J. Cell Sci. 117*, 2449−2460.
6. Kung, C. (2005) A possible unifying principle for mechanosensation, *Nature 436*, 647−654.
7. Perozo, E. (2006) Gating prokaryotic mechanosensitive channels, *Nat. Rev. Mol. Cell Biol. 7*, 109−119.
8. Patel, A. J., Honore, E., Maingret, F., Lesage, F., Fink, M., Duprat, F., and Lazdunski, M. (1998) A mammalian two pore domain mechano-gated S-like K^+ channel, *EMBO J. 17*, 4283−4290.
9. Maingret, F., Patel, A. J., Lesage, F., Lazdunski, M., and Honore, E. (1999) Mechano- or acid stimulation, two interactive modes of activation of the TREK-1 potassium channel, *J. Biol. Chem. 274*, 26691−26696.
10. Kellenberger, S., and Schild, L. (2002) Epithelial sodium channel/degenerin family of ion channels: A variety of functions for a shared structure, *Physiol. Rev. 82*, 735−767.
11. Corey, D. P. (2003) New TRP channels in hearing and mechanosensation, *Neuron 39*, 585−588.
12. Berrier, C., Besnard, M., Ajouz, B., Coulombe, A., and Ghazi, A. (1996) Multiple mechanosensitive ion channels from *Escherichia coli*, activated at different thresholds of applied pressure, *J. Membr. Biol. 151*, 175−187.
13. Levina, N., Totemeyer, S., Stokes, N. R., Louis, P., Jones, M. A., and Booth, I. R. (1999) Protection of *Escherichia coli* cells against extreme turgor by activation of MscS and MscL mechanosensitive channels: Identification of genes required for MscS activity, *EMBO J. 18*, 1730−1737.
14. Batiza, A. F., Kuo, M. M., Yoshimura, K., and Kung, C. (2002) Gating the bacterial mechanosensitive channel MscL *in vivo*, *Proc. Natl. Acad. Sci. U.S.A. 99*, 5643−5648.
15. Martinac, B., Buechner, M., Delcour, A. H., Adler, J., and Kung, C. (1987) Pressure-sensitive ion channel in *Escherichia coli*, *Proc. Natl. Acad. Sci. U.S.A. 84*, 2297−2301.
16. Sukharev, S. I., Martinac, B., Arshavsky, V. Y., and Kung, C. (1993) Two types of mechanosensitive channels in the *Escherichia coli* cell envelope: Solubilization and functional reconstitution, *Biophys. J. 65*, 177−183.
17. Koprowski, P., and Kubalski, A. (1998) Voltage-independent adaptation of mechanosensitive channels in *Escherichia coli* protoplasts, *J. Membr. Biol. 164*, 253−262.
18. Perozo, E., Cortes, D. M., Sompornpisut, P., Kloda, A., and Martinac, B. (2002) Open channel structure of MscL and the gating mechanism of mechanosensitive channels, *Nature 418*, 942−948.
19. Chang, G., Spencer, R. H., Lee, A. T., Barclay, M. T., and Rees, D. C. (1998) Structure of the MscL homolog from *Mycobacterium tuberculosis*: A gated mechanosensitive ion channel, *Science 282*, 2220−2226.
20. Bass, R. B., Strop, P., Barclay, M., and Rees, D. C. (2002) Crystal structure of *Escherichia coli* MscS, a voltage-modulated and mechanosensitive channel, *Science 298*, 1582−1587.
21. Pivetti, C. D., Yen, M. R., Miller, S., Busch, W., Tseng, Y. H., Booth, I. R., and Saier, M. H., Jr. (2003) Two families of mechanosensitive channel proteins, *Microbiol. Mol. Biol. Rev. 67*, 66−85.
22. Kloda, A., and Martinac, B. (2002) Common evolutionary origins of mechanosensitive ion channels in Archaea, Bacteria and cell-walled Eukarya, *Archaea 1*, 35−44.
23. Haswell, E. S., and Meyerowitz, E. M. (2006) MscS-like proteins control plastid size and shape in *Arabidopsis thaliana*, *Curr. Biol. 16*, 1−11.
24. Langton, P. D. (1993) Calcium channel currents recorded from isolated myocytes of rat basilar artery are stretch sensitive, *J. Physiol. 471*, 1−11.
25. Jennings, L. J., Xu, Q. W., Firth, T. A., Nelson, M. T., and Mawe, G. M. (1999) Cholesterol inhibits spontaneous action potentials and calcium currents in guinea pig gallbladder smooth muscle, *Am. J. Physiol. 277*, G1017−G1026.
26. Calabrese, B., Tabarean, I. V., Juranka, P., and Morris, C. E. (2002) Mechanosensitivity of N-type calcium channel currents, *Biophys. J. 83*, 2560−2574.
27. Laitko, U., Juranka, P. F., and Morris, C. E. (2006) Membrane stretch slows the concerted step prior to opening in a Kv channel, *J. Gen. Physiol. 127*, 687−701.
28. Cortes, D. M., and Perozo, E. (1997) Structural dynamics of the *Streptomyces lividans* K^+ channel (SKC1): Oligomeric stoichiometry and stability, *Biochemistry 36*, 10343−10352.
29. Perozo, E., Cortes, D. M., and Cuello, L. G. (1998) Three-dimensional architecture and gating mechanism of a K^+ channel studied by EPR spectroscopy, *Nat. Struct. Biol. 5*, 459−469.
30. Cortes, D. M., Cuello, L. G., and Perozo, E. (2001) Molecular architecture of full-length KcsA: Role of cytoplasmic domains in ion permeation and activation gating, *J. Gen. Physiol. 117*, 165−180.
31. Sukharev, S. (2002) Purification of the small mechanosensitive channel of *Escherichia coli* (MscS): The subunit structure, conduction, and gating characteristics in liposomes, *Biophys. J. 83*, 290−298.
32. Sotomayor, M., Vasquez, V., Perozo, E., and Schulten, K. (2007) Ion Conduction through MscS as Determined by Electrophysiology and Simulation, *Biophys. J. 92*, 886−902.
33. Cuello, L. G., Cortes, D. M., and Perozo, E. (2004) Molecular architecture of the KvAP voltage-dependent K^+ channel in a lipid bilayer, *Science 306*, 491−495.
34. Miller, S., Bartlett, W., Chandrasekaran, S., Simpson, S., Edwards, M., and Booth, I. R. (2003) Domain organization of the MscS mechanosensitive channel of *Escherichia coli*, *EMBO J. 22*, 36−46.
35. Miller, S., Edwards, M. D., Ozdemir, C., and Booth, I. R. (2003) The closed structure of the MscS mechanosensitive channel. Cross-linking of single cysteine mutants, *J. Biol. Chem. 278*, 32246−32250.
36. Schumann, U., Edwards, M. D., Li, C., and Booth, I. R. (2004) The conserved carboxy-terminus of the MscS mechanosensitive channel is not essential but increases stability and activity, *FEBS Lett. 572*, 233−237.
37. Strop, P., and Brunger, A. T. (2005) Refractive index-based determination of detergent concentration and its application to the study of membrane proteins, *Protein Sci. 14*, 2207−2211.
38. Akitake, B., Anishkin, A., and Sukharev, S. (2005) The "dashpot" mechanism of stretch-dependent gating in MscS, *J. Gen. Physiol. 125*, 143−154.
39. Encinar, J. A., Molina, M. L., Poveda, J. A., Barrera, F. N., Renart, M. L., Fernandez, A. M., and Gonzalez-Ros, J. M. (2005) The influence of a membrane environment on the structure and stability of a prokaryotic potassium channel, KcsA, *FEBS Lett. 579*, 5199−5204.
40. Farahbakhsh, Z. T., Altenbach, C., and Hubbell, W. L. (1992) Spin labeled cysteines as sensors for protein-lipid interaction and conformation in rhodopsin, *Photochem. Photobiol. 56*, 1019−1033.
41. McHaourab, H. S., Hyde, J. S., and Feix, J. B. (1994) Binding and state of aggregation of spin-labeled cecropin AD in phospholipid bilayers: Effects of surface charge and fatty acyl chain length, *Biochemistry 33*, 6691−6699.
42. Perozo, E., Kloda, A., Cortes, D. M., and Martinac, B. (2001) Site-directed spin-labeling analysis of reconstituted Mscl in the closed state, *J. Gen. Physiol. 118*, 193−206.
43. Perozo, E., Kloda, A., Cortes, D. M., and Martinac, B. (2002) Physical principles underlying the transduction of bilayer deformation forces during mechanosensitive channel gating, *Nat. Struct. Biol. 9*, 696−703.
44. Stokes, N. R., Murray, H. D., Subramaniam, C., Gourse, R. L., Louis, P., Bartlett, W., Miller, S., and Booth, I. R. (2003) A role for mechanosensitive channels in survival of stationary phase: Regulation of channel expression by RpoS, *Proc. Natl. Acad. Sci. U.S.A. 100*, 15959−15964.
45. Akitake, B., Spelbrink, R. E., Anishkin, A., Killian, J. A., de Kruijff, B., and Sukharev, S. (2007) 2,2,2-Trifluoroethanol changes the transition kinetics and subunit interactions in the small bacterial mechanosensitive channel MscS, *Biophys. J.* (in press).
46. Lemmon, M. A., Flanagan, J. M., Hunt, J. F., Adair, B. D., Bormann, B. J., Dempsey, C. E., and Engelman, D. M. (1992) Glycophorin A dimerization is driven by specific interactions between transmembrane α-helices, *J. Biol. Chem. 267*, 7683−7689.
47. Martinac, B., Adler, J., and Kung, C. (1990) Mechanosensitive ion channels of *E. coli* activated by amphipaths, *Nature 348*, 261−263.

BI700322K